Selectivity of the $^{16}O(e,e'pp)$ reaction to discrete final states

C. Giusti and F. D. Pacati
Dipartimento di Fisica Nucleare e Teorica dell'Università, Pavia and Istituto Nazionale di Fisica Nucleare, Sezione di Pavia, Italy

K. Allaart and W. J. W. Geurts
Department of Physics and Astronomy, Vrije Universiteit, De Boelelaan 1081, 1081 HV Amsterdam, The Netherlands

W. H. Dickhoff
Department of Physics, Washington University, St. Louis, Missouri 63130

H. Müther
Institut für Theoretische Physik, Universität Tübingen, Auf der Morgenstelle 14, D-72076 Tübingen, Germany
(Received 9 September 1997)

Resolution of discrete final states in the $^{16}O(e,e'pp)^{14}C$ reaction may provide an interesting tool to discriminate between contributions from one- and two-body currents in this reaction. This is based on the observation that the 0^+ ground state and first 2^+ state of ^{14}C are reached predominantly by the removal of a $^1S_0$ pair from ^{16}O in this reaction, whereas other states mostly arise by the removal of a ^3P pair. This theoretical prediction has been supported recently by an analysis of the pair momentum distribution of the experimental data [1]. In this paper we present results of reaction calculations performed in a direct knockout framework where final-state interaction and one- and two-body currents are included. The two-nucleon overlap integrals are obtained from a calculation of the two-proton spectral function of ^{16}O and include both long-range and short-range correlations. The kinematics chosen in the calculations is relevant for recent experiments at NIKHEF and Mainz. We find that the knockout of a ^3P proton pair is largely due to the (two-body) Δ current. The $^1S_0$ pair knockout, on the other hand, is dominated by contributions from the one-body current and therefore sensitive to two-body short-range correlations. This opens up good perspectives for the study of these correlations in the $^{16}O(e,e'pp)$ reaction involving the lowest few states in ^{14}C. In particular the longitudinal structure function f_{00}, which might be separated with superparallel kinematics, turns out to be quite sensitive to the NN potential that is adopted in the calculations. [S0556-2813(98)00904-2]

PACS number(s): 21.60.−n, 21.10.Jx, 21.30.Fe, 25.30.Fj

I. INTRODUCTION

Exclusive $(e,e'pp)$ reactions on nuclei have recently been added to the rich set of tools exploring the nucleus with the electromagnetic interaction [1]. It is hoped that this new tool may contribute to clarification of the nature and influence of short-range correlations (SRC) in low-energy nuclear phenomena. Several early theoretical papers [2,3] established a link between two-nucleon removal cross sections and the two-nucleon density matrix [2] or the two-nucleon spectral function [3] which contain information related to SRC. A somewhat different perspective on this issue has been explored in Refs. [4,5]. The anticipated availability of this reaction generated renewed theoretical interest [6–8] in the reaction description on the one hand, and in the calculation of the two-nucleon spectral function on the other. Several groups have developed a description of two-nucleon emission processes induced by photons or electrons [8–19]. Indeed, it appears from these studies that the most promising reaction to study short-range phenomena involves the $(e,e'pp)$ channel, where the effect of meson-exchange currents and Δ isobars is less dominant as compared to the $(e,e'pn)$ and (γ,NN) processes.

Although the $(e,e'pp)$ reaction has been calculated for light nuclei [20], these nuclei lack specific final states that may act as a filter for the study of various reaction processes. The presence of discrete final states with well-defined angular momentum makes ^{16}O a more attractive target. After the initial exploratory experiments at NIKHEF on ^{12}C [21,22] where it was demonstrated that such difficult experiments are indeed feasible, further studies have concentrated on ^{16}O at two major electron accelerators, the AmPS-facility at NIKHEF-Amsterdam [1] and the MAMI-facility in Mainz [23]. At both these facilities it has been possible to achieve sufficient resolution to allow the separation of the cross section related to distinct states or groups of final states of ^{14}C. A further experiment on ^{16}O with improved statistics has been recently approved in Mainz [24].

In this work we will employ the reaction description of Ref. [12]. This description of the $(e,e'pp)$ excitation process includes the contribution of the usual one-body terms as well as those two-body currents which involve the intermediate excitation of the Δ isobar. The deexcitation of the Δ after absorption of the photon or the excitation of the Δ before absorption of the photon proceeds by exchange of a pion with another nucleon. In the present work an improvement of the dynamic aspects of the propagation of the Δ isobar is taken into account [25]. A treatment of Δ propaga-

tion involving the exchange of rho mesons is not included at present. The treatment of the final state interaction of the outgoing protons with the remaining nucleus is treated by neglecting their mutual interaction but including the distorting effect of their interaction with the remaining nucleons in terms of an optical potential. The latter distortion of the individual protons is constrained by experimental data obtained from elastic scattering of nucleons off nuclei. The approximation to neglect the interaction between the two outgoing protons has been justified in the past by arguing that the pair of protons will leave the nucleus largely back to back making this type of final state interaction less important. This issue should be further studied in the future since there is no *a priori* dominance of the effects of correlations before or after the absorption of the photon as emphasized in Ref. [5]. It is, however, possible that angular momentum and parity restrictions associated with the transition to specific discrete final states in the remaining nucleus may filter the importance of this type of final state interaction.

Essentially all published work on the description of the $(e,e'pp)$ reaction employs a relatively simple description of the nuclear structure of the target nucleus. While SRC are modeled and included at the level of a central correlation function taken mostly from nuclear matter calculations and sometimes involving semirealistic interactions, a consistent treatment of the low-energy shell-model structure together with attendant inclusion of SRC has not been available so far in the description of initial state correlations. The critical information about SRC in the transition to the final A-2 state is incorporated in the two-body spectral function at the corresponding energy. At low missing energy, it represents the probability density for the removal of a pair of nucleons (protons in the present work) from the ^{16}O ground state to a specific discrete final state in ^{14}C. Since this removal amplitude involves nucleons close to the Fermi energy, the accurate description of this process requires a careful treatment of the influence of low-energy, or long-range, correlations associated with the soft-surface features of the ^{16}O nucleus. The latter feature has not been included in Ref. [12], but is incorporated in Ref. [26]. It is the purpose of the present work to combine the reaction description of the two-proton removal process of Ref. [12] with the many-body calculation of the two-particle spectral function in ^{16}O of Ref. [26] in order to calculate cross sections for the triple-coincidence experiments performed at NIKHEF and Mainz.

The calculation of the two-body spectral function in Ref. [26] includes the dressing of individual nucleons through their coupling to low-lying core excitations. In addition, the reduced presence of these nucleons at low energy associated with strength removal due to the influence of SRC is incorporated [28]. This yields theoretical spectroscopic factors for low-lying states in ^{15}N which represent the closest agreement with experiment [29] to date. Consistency between the two aspects of the calculations (long-range vs short-range) is ensured by employing the same effective interaction (G-matrix) in the calculation of the long-range correlations which is responsible for the removal of single-particle strength. Although the appearance of high-momentum nucleons in the ground state is implied by SRC, their presence is only apparent at high excitation energy in the A-1 system [30,31]. The corresponding cross section for the removal of high-momentum protons from ^{16}O in the $(e,e'p)$ reaction has recently been calculated in Ref. [32]. Although these cross sections are large enough to be detectable at these high energies, other competing processes will also be present making a clear-cut identification of SRC in the $(e,e'p)$ reaction difficult.

This elusive consequence of SRC in the $(e,e'p)$ reaction does not pertain to the removal of a pair of nucleons leading to a discrete final state in the A-2 system since few other competing processes are present. The strongly reduced probability for a pair of protons to be in close proximity will unavoidably lead to the presence of high-momentum components in their relative momentum wave function. The character and strength of these high-momentum components depends on certain aspects of short-range phenomena which are described differently by different nucleon-nucleon (NN) interactions. Sensitivity to the choice of the NN interaction in describing pairs with high relative momentum in the two-body spectral function has been established in Ref. [26]. It is hoped that a realistic treatment of the reaction process combined with a detailed many-body treatment of the spectral function in conjunction with new experimental data may contribute to a clear and unambiguous determination of SRC in nuclei.

The possibility to analyze different final states in the reaction has already been explored in Ref. [12]. As discussed above, the separation of some of the low-lying final states has recently been realized experimentally at the NIKHEF [1] and Mainz [23] facilities. In the present work we attempt to identify those transitions that are strongly influenced by SRC and those where two-body transition currents play a dominant role. This feature makes the ^{16}O nucleus a prime candidate for such an analysis, unlike the ^{4}He nucleus which does not yield any bound states upon the removal of two protons. In Sec. II of this paper the essential ingredients of the description of the $(e,e'pp)$ reaction and the calculation of the two-particle spectral function are summarized. The results are discussed in Sec. III, while conclusions are drawn in Sec. IV.

II. CALCULATION OF THE $(e,e'pp)$ CROSS SECTION

A. Reaction mechanism

The triple coincidence cross section for the reaction induced by an electron, with momentum $\boldsymbol{p}_0$, where two nucleons, with momenta $\boldsymbol{p}'_1$ and $\boldsymbol{p}'_2$, are ejected from a nucleus is given, in the one-photon exchange approximation, by the contraction between a lepton and a hadron tensor. If the effect of the nuclear Coulomb field on the incident and the outgoing electrons is neglected, the Lorentz condition for the Möller potential and the continuity equation for the hadronic current make it possible to separate the longitudinal and transverse components of the interaction and to write the cross section as a linear combination of independent structure functions. For an unpolarized electron, after integration over the energy of one of the emitted nucleons (E'_2), the cross section is expressed in terms of six structure functions as [9–11],

$$\frac{d^8\sigma}{dp_0'd\Omega_0'dE_1'd\Omega_1'd\Omega_2'}=\frac{\pi e^2}{2q}\Gamma_V\Omega_f f_{rec}[2\epsilon_L f_{00}+f_{11}$$
$$-\epsilon(f_{1-1}\cos 2\alpha+\overline{f}_{1-1}\sin 2\alpha)$$
$$+\sqrt{\epsilon_L(1+\epsilon)}(f_{01}\cos\alpha$$
$$+\overline{f}_{01}\sin\alpha)], \quad (1)$$

where $e^2/4\pi\simeq 1/137$, $\boldsymbol{p}_0'$ is the momentum of the scattered electron, and α is the angle between the plane of the electrons and the plane containing the momentum transfer $\boldsymbol{q}$ and $\boldsymbol{p}_1'$. The quantity

$$\epsilon=\left(1-\frac{2\boldsymbol{q}^2}{q_\mu^2}\tan^2\frac{\theta}{2}\right)^{-1} \quad (2)$$

measures the polarization of the virtual photon exchanged by the electron scattered at an angle θ and

$$\epsilon_L=-\frac{q_\mu^2}{\boldsymbol{q}^2}\epsilon, \quad (3)$$

where $q_\mu^2=\omega^2-\boldsymbol{q}^2$, with $\omega=p_0-p_0'$ and $\boldsymbol{q}=\boldsymbol{p}_0-\boldsymbol{p}_0'$, is the four-momentum transfer. The factor

$$\Gamma_V=\frac{e^2}{8\pi^3}\frac{p_0'}{p_0}\frac{q}{q_\mu^2}\frac{1}{\epsilon-1}, \quad (4)$$

is the flux of virtual photons, $\Omega_f=p_1'E_1'p_2'E_2'$ is the phase-space factor, and

$$f_{rec}^{-1}=1-\frac{E_2'}{E_B}\frac{\boldsymbol{p}_2'\cdot\boldsymbol{p}_B}{\boldsymbol{p}_2'^2} \quad (5)$$

is the inverse of the recoil factor. The quantity E_B is the total relativistic energy of the residual nucleus with momentum $\boldsymbol{p}_B=\boldsymbol{q}-\boldsymbol{p}_1'-\boldsymbol{p}_2'$.

The structure functions $f_{\lambda\lambda'}$ represent the response of the nucleus to the longitudinal ($\lambda=0$) and transverse ($\lambda=\pm1$) components of the electromagnetic interaction and only depend on ω, q, p_1' p_2' and the angles γ_1 between $\boldsymbol{q}$ and $\boldsymbol{p}_1'$, γ_2 between $\boldsymbol{q}$ and $\boldsymbol{p}_2'$, and γ_{12} between $\boldsymbol{p}_1'$ and $\boldsymbol{p}_2'$ [9]. They result from suitable combinations of the components of the hadron tensor [9,11] and are thus given by bilinear combinations of the Fourier transforms of the transition matrix elements of the nuclear charge-current density operator taken between initial and final nuclear states

$$J^\mu(\boldsymbol{q})=\int\langle\Psi_f|\hat{J}^\mu(\boldsymbol{r})|\Psi_i\rangle e^{i\boldsymbol{q}\cdot\boldsymbol{r}}d\boldsymbol{r}. \quad (6)$$

These integrals represent the basic ingredients of the calculation.

If the residual nucleus is left in a discrete eigenstate of its Hamiltonian, i.e., for an exclusive process, and under the assumption of a direct knockout mechanism, the matrix elements of Eq. (6) can be written as [9,12]

$$J^\mu(\boldsymbol{q})=\int\psi_f^*(\boldsymbol{r}_1\boldsymbol{\sigma}_1,\boldsymbol{r}_2\boldsymbol{\sigma}_2)J^\mu(\boldsymbol{r},\boldsymbol{r}_1\boldsymbol{\sigma}_1,\boldsymbol{r}_2\boldsymbol{\sigma}_2)$$
$$\times\psi_i(\boldsymbol{r}_1\boldsymbol{\sigma}_1,\boldsymbol{r}_2\boldsymbol{\sigma}_2)e^{i\boldsymbol{q}\cdot\boldsymbol{r}}d\boldsymbol{r}d\boldsymbol{r}_1d\boldsymbol{r}_2d\boldsymbol{\sigma}_1d\boldsymbol{\sigma}_2. \quad (7)$$

Equation (7) contains three main ingredients: the final-state wave function ψ_f, the nuclear current J^μ, and the two-nucleon overlap integral ψ_i. The derivation of Eq. (7) involves bound and scattering states ψ_i and ψ_f which are consistently derived from an energy-dependent non-Hermitian Feshbach-type Hamiltonian for the considered final state of the residual nucleus. They are eigenfunctions of this Hamiltonian at negative and positive energy eigenvalues, respectively [9,11]. In practice, it is not possible to achieve this consistency and the treatment of initial and final state correlations proceeds separately with different approximations.

The same theoretical model for the exclusive $(e,e'pp)$ reaction as in Ref. [12] is used, but here an improved treatment of the nuclear current and of the two-nucleon overlap integral has been adopted, as described below. In the final-state wave function ψ_f each of the outgoing nucleons interacts with the residual nucleus while the mutual interaction between the two outgoing nucleons is neglected. The scattering state is thus written as the product of two uncoupled single-particle distorted wave functions, eigenfunctions of a complex phenomenological optical potential which contains a central, a Coulomb, and a spin-orbit term. The effects of an isospin-dependent term, to account for charge-exchange final-state interactions, were evaluated for the $(e,e'pp)$ reaction in Ref. [13] but negligible contributions were obtained in all the situations of practical interest. Thus this term is neglected here.

The nuclear current J^μ is the sum of a one-body and a two-body part. The one-body part contains a Coulomb, a convective, and a spin term. The two-body component is derived from the effective Lagrangian of Ref. [33], performing a nonrelativistic reduction of the lowest order Feynman diagrams with one-pion exchange. In this approximation only processes with Δ-isobar configurations in the intermediate state contribute to the $(e,e'pp)$ reaction. They produce a completely transverse current, $\boldsymbol{J}^\Delta$. The operator form of $\boldsymbol{J}^\Delta$ was derived in Ref. [25]. It results from the sum of the contributions due to two types of processes, corresponding to the excitation and deexcitation part of the current. In the former case, the Δ is excited by photon absorption and then deexcited by pion exchange. The latter process describes the time interchange of the two steps, i.e., first excitation of a virtual Δ by pion exchange in a NN collision and subsequent deexcitation by photon absorption. For a pp pair they give [25]

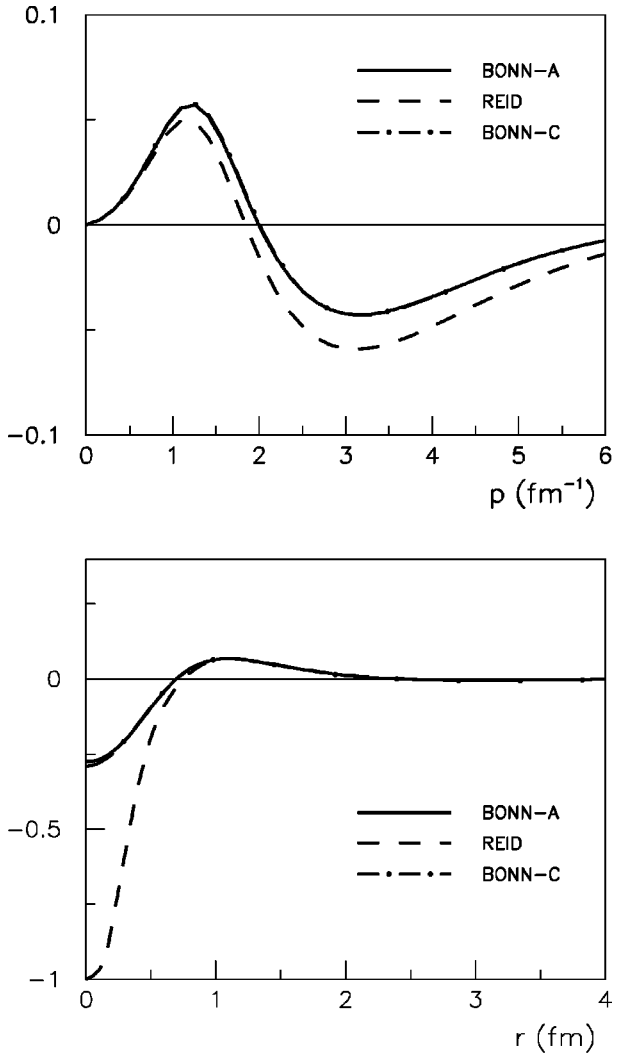

FIG. 1. Defect functions [see Eq. (15)] in momentum space (top), multiplied by $p=|\boldsymbol{p}_1-\boldsymbol{p}_2|/2$, and coordinate space (bottom) calculated for the $^1S_0$ partial wave by solving the Bethe-Goldstone equation in ^{16}O, by the method of Ref. [38]. Results are plotted for the Bonn-A, Bonn-C, and Reid Soft Core potential.

$$\boldsymbol{J}^{\Delta}_{\mathrm{I,II}}(\boldsymbol{q},\boldsymbol{\sigma}_1,\boldsymbol{\sigma}_2)=\frac{1}{9}\gamma 2\boldsymbol{\tau}^{(2)}_3(2i\boldsymbol{k}\mp\boldsymbol{k}\times\boldsymbol{\sigma}^{(1)}) \times\boldsymbol{q}G_{\Delta}(\sqrt{s_{\mathrm{I,II}}})\,\frac{\boldsymbol{\sigma}^{(2)}\cdot\boldsymbol{k}}{\boldsymbol{k}^2+m^2}F(q^2_{\mu})+(1\leftrightarrow 2), \tag{8}$$

where $\boldsymbol{k}$ is the momentum of the exchanged pion, m is the pion mass, and the factor γ collects various coupling constants, $\gamma=f_{\gamma N\Delta}f_{\pi NN}f_{\pi N\Delta}/m^3$. The dipole form factor

$$F(q^2_{\mu})=\left[1-\frac{q^2_{\mu}}{(855\ \mathrm{MeV})^2}\right]^{-2} \tag{9}$$

takes into account the electromagnetic form factor of the isobar, which corresponds to the isovector form factor $G^{\mathrm{V}}_{\mathrm{M}}$ used in the static quark model [34]. The propagator of the resonance, G_{Δ}, depends on the invariant energy $\sqrt{s}$ of the Δ, which is different for parts I and II. For the deexcitation current $\sqrt{s_{\mathrm{II}}}$ is approximated by the nucleon mass M and

$$G_{\Delta}=(M_{\Delta}-M)^{-1}, \tag{10}$$

where $M_{\Delta}=1232$ MeV. For the excitation current we use [35]

$$\sqrt{s_{\mathrm{I}}}=\sqrt{s_{NN}}-M, \tag{11}$$

where $\sqrt{s_{NN}}$ is the experimentally measured invariant energy of the two outgoing nucleons. This gives

TABLE I. Two-proton removal amplitudes from ^{16}O for states of ^{14}C that are expected to be strongly populated in the ^{16}O$(e,e'pp)$ reaction. These are based on the dressed RPA calculations described in Ref. [26], within a model space of the $0s$ up to the $1p0f$ shells and with the G-matrix derived from the Bonn-C potential as an effective interaction. The quantum number ρ is the total number of harmonic oscillator quanta of the pair: $\rho=2n+l+2N+L$ (lower case for relative and upper case for center of mass motion). For instance $\rho=4$ indicates contributions from the sd shell and $\rho=6$ from the pf shell. The energies of the listed states are largely known from experiments: 0^+_1 represents the ground state of ^{14}C, 2^+_1 represents the sum of the 2^+ states at 7.01 and 8.32 MeV [44], and the 1^+ is known [44] at 11.3 MeV. The 2^+_2 was identified with a bump around 16 MeV observed in Ref. [1]. The location of the 0^+_2 is less clear; the strength may be fragmented over several final states in the range between 12 and 14 MeV [1].

	n	N	ρ	0^+_1	0^+_2
$^1S_0;\ L=0$	0	1	2	−0.416	−0.374
	1	0	2	+0.416	+0.374
	0	0	0	+0.057	+0.081
	1	1	4	−0.073	−0.040
	0	2	4	+0.040	+0.022
	2	0	4	+0.040	+0.022
	1	2	6	+0.016	+0.010
	2	1	6	−0.016	−0.010
$^3P_1;\ L=1$	0	0	2	+0.507	−0.561
	0	1	4	+0.025	−0.006
	1	0	4	−0.025	+0.006
$^1D_2;\ L=2$	0	0	4	+0.016	+0.008
	n	N	ρ	2^+_1	2^+_2
$^1S_0;\ L=2$	0	0	2	+0.489	+0.256
	1	0	4	+0.017	+0.007
	0	1	4	−0.011	−0.005
$^3P_1;\ L=1$	0	0	2	−0.177	+0.338
$^3P_2;\ L=1$	0	0	2	−0.307	+0.586
$^1D_2;\ L=0$	0	0	2	−0.489	−0.256
	0	1	4	+0.017	+0.007
	1	0	4	−0.011	−0.005
	n	N	ρ	1^+	
$^3P_0;\ L=1$	0	0	2	+0.444	
$^3P_1;\ L=1$	0	0	2	+0.384	
$^3P_2;\ L=1$	0	0	2	−0.496	

$$G_\Delta(\sqrt{s_I})=\left(M_\Delta-\sqrt{s_I}-\frac{i}{2}\Gamma_\Delta(\sqrt{s_I})\right)^{-1}, \quad (12)$$

where the decay width of the Δ, Γ_Δ has been taken in the calculations according to the parametrization of Ref. [36].

The two-nucleon overlap integral ψ_i in (7) contains the information on nuclear structure. For a discrete final state of the ^{14}C nucleus, with angular momentum quantum numbers JM, the relevant part may be expressed in terms of relative and center-of-mass (c.m.) wave functions as

$$\psi_i(\boldsymbol{r}_1\boldsymbol{\sigma}_1,\boldsymbol{r}_2\boldsymbol{\sigma}_2)=\sum_{nlSjNL} c^i_{nlSjNL}\phi_{nlSj}(r)R_{NL}(R) \times[\mathcal{F}^j_{lS}(\Omega_r,\boldsymbol{\sigma}_1,\boldsymbol{\sigma}_2)Y_L(\Omega_R)]^{JM}, \quad (13)$$

where

$$\boldsymbol{r}=\boldsymbol{r}_1-\boldsymbol{r}_2, \quad \boldsymbol{R}=\frac{\boldsymbol{r}_1+\boldsymbol{r}_2}{2} \quad (14)$$

are the relative and c.m. variables. Note that we follow the convention to denote lower case for relative and upper case for c.m. coordinate quantum numbers. In addition, we note that the oscillator parameter $b=1.7677$ fm for the sp oscillator states has been used. The brackets in (13) indicate angular momentum coupling of the angular and spin wave function $\mathcal{F}$ of relative motion with the spherical harmonic of the c.m. coordinate to the total angular momentum quantum numbers JM. The c.m. radial wave function R is that of a harmonic oscillator [37], but the radial wave function ϕ of relative motion includes a defect function in order to account for SRC [26]

$$\phi_{nlSj}(r)=R_{nl}(r)+D_{lSj}(r). \quad (15)$$

These defect wave functions were obtained by solving the Bethe-Goldstone equation in momentum space for ^{16}O [38]. For the present application these defect functions were Fourier Bessel transformed into coordinate space. This is not an exact procedure; the solution of the Bethe-Goldstone equation yields a nonlocal correlation operator which cannot strictly be represented by a local correlation function D_{lSj} of the form displayed in Eq. (15). However, for the $^1S_0$ wave, which is decoupled from other partial waves, the approximation is quite satisfactory. The evaluation of the defect wave function in this partial wave of relative motion is rather insensitive to the quantum numbers of the two-particle state in the inertial system of the nucleus, for which it is determined. For the higher partial waves of the pp wave function the effect of SRC is relatively small due to the presence of centrifugal terms.

The defect functions for the $^1S_0$ partial wave are displayed in Fig. 1 for the Bonn-A, Bonn-C, and Reid Soft Core potentials both as a function of relative momentum and relative distance. One of the objectives of the present study is to investigate to what extent the differences between these defect functions are reflected in the calculated cross sections.

The coefficients c in Eq. (13) contain contributions from a shell-model space which includes the $0s$ up to the $1p0f$ shells. The framework within which this is done is basically the same as the one adopted in a recent calculation of the two-proton removal spectral function in momentum space [26]. The main ingredients of this method are briefly presented in the next subsection.

B. Structure amplitudes

The guiding principle followed in the calculation of the structure amplitudes, which was presented earlier in Ref. [26], is the attempt of treating long-range and short-range correlations in a separate but consistent way. The effects of long-range correlations are determined by performing a nuclear structure calculation within a shell-model space including single-particle states which range from the $0s$ up to the $1p0f$ shell. Thus the expansion in Eq. (13) is limited to configurations within this model space of two major shells above and two major shells below the Fermi level. The calculated amplitudes, cf. Table I, indicate that the two-nucleon removal transitions are not very collective, in other words they are not made up of many components of comparable magnitude. The only exception may be the ground state to ground state transition where the strong pairing component of the interaction may slightly further enhance the transition strength by coherent contributions from higher shells. Although the treatment of long-range correlations for the sp strength is not complete, extension of the model space to include more shells is unlikely to lead to further improvements [27].

The effects of the strong short-range components of a realistic NN interaction, which would scatter the interacting nucleons into much higher shells, are taken into account by solving the Bethe-Goldstone equation using a Pauli operator which considers only configurations outside this model space. The distinction between long-range (inside the model space) and short-range correlations (outside the model space) is an artificial one. However, it is important to treat those contributions consistently and to avoid any kind of double counting. This is an important merit of the present approach. The solution of this Bethe-Goldstone equation yields the residual interaction of the nucleons inside the model space as well as the defect functions employed in Eq. (15). The depletion of filled orbits by SRC is also incorporated in the shell-model space calculation by the energy dependence of the G-matrix interaction, which yields an energy dependent Hartree-Fock term in the self-energy [28]. The fragmentation of one-nucleon removal strength is described by two-particle–one-hole and two-hole–one-particle terms in the self-energy Σ^* in Tamm-Dancoff approximation [28,39], with which the Dyson equation for the one-body propagator

$$g_{\alpha\beta}(\omega)=g^0_{\alpha\beta}(\omega)+\sum_{\gamma\delta} g^0_{\alpha\gamma}(\omega)\Sigma^*_{\gamma\delta}(\omega)g_{\delta\beta}(\omega) \quad (16)$$

is solved. In Ref. [28] these dressed propagators were used to calculate the one-nucleon removal spectroscopic factors for the low-energy final states in ^{15}N. The comparison with the results of one-nucleon knockout experiments is then a first test of the quality of this ingredient in the calculation of two-nucleon removal amplitudes. The latter are contained in the Lehmann representation of the two-nucleon propagator $G^{\rm II}$

$$G^{\rm II}_{abcd;J}(\omega)=\sum_n \frac{\langle\Psi_0^A\|(a_\beta a_\alpha)_J\|\Psi_J^{n,A+2}\rangle\langle\Psi_J^{n,A+2}\|(a_\gamma^\dagger a_\delta^\dagger)_J\|\Psi_0^A\rangle}{\omega-(E_J^{n,A+2}-E^{0,A})+i\eta}-\sum_m \frac{\langle\Psi_0^A\|(a_\gamma^\dagger a_\delta^\dagger)_J\|\Psi_J^{m,A-2}\rangle\langle\Psi_J^{m,A-2}\|(a_\beta a_\alpha)_J\|\Psi_0^A\rangle}{\omega-(E^{0,A}-E_J^{m,A-2})-i\eta}$$

$$=\sum_n \frac{Y^{n*}_{abJ}Y^n_{cdJ}}{\omega-(E_J^{n,A+2}-E^{0,A})+i\eta}-\sum_m \frac{X^{m*}_{cdJ}X^m_{abJ}}{\omega-(E^{0,A}-E_J^{m,A-2})-i\eta}. \tag{17}$$

The symbols $\langle\cdots\|\cdots\|\cdots\rangle$ represent the reduced matrix elements [40–42] of the two-nucleon removal and addition tensor operators that are constructed by the angular momentum coupling of two one-nucleon addition and removal tensors $a_\alpha^\dagger$ and $a_{\tilde\alpha}$, where $a_{\tilde\alpha}=(-)^{j_\alpha-m_\alpha}a_{-\alpha}$ is the time reverse of α; $-\alpha$ denotes $\{n_\alpha,l_\alpha,j_\alpha,-m_\alpha\}$ and a denotes basis states without the magnetic quantum number: $a=\{n_\alpha,l_\alpha,j_\alpha\}$.

The two-nucleon propagator is obtained by solving, within the shell-model space, the Bethe-Salpeter equation [42,43] for the two-nucleon propagator $G^{\rm II}$

$$G^{\rm II}_{\alpha\beta\gamma\delta}(t_1,t_2,t_3,t_4)=i[g_{\alpha\gamma}(t_1-t_3)g_{\beta\delta}(t_2-t_4)-g_{\alpha\delta}(t_1-t_4)g_{\beta\gamma}(t_2-t_3)]-\int_{-\infty}^{\infty}dt_1'dt_2'dt_3'dt_4'\sum_{\mu\nu\kappa\lambda}[g_{\alpha\mu}(t_1-t_1')$$
$$\times g_{\beta\nu}(t_2-t_2')]\Gamma^{pp}_{\mu\nu\kappa\lambda}(t_1',t_2',t_3',t_4')G^{\rm II}_{\kappa\lambda\gamma\delta}(t_3',t_4',t_3,t_4), \tag{18}$$

where Γ denotes the irreducible effective particle-particle interaction, which is here approximated by the G-matrix interaction which contains only propagation of particles outside the chosen model space.

In the calculation of Ref. [28] the spectroscopic factor for the removal of *one* nucleon from the p shell of ^{16}O turned out to be reduced by a factor 0.75 as compared with the independent-particle shell model. This is still about 10% larger than the factor 0.65 deduced from experiments [29]. We decided not to replace the calculated spectroscopic factor by the experimental ones in the dressed propagators. This means that the *two*-nucleon removal amplitudes that we obtain in the RPA with these dressed propagators [26] may be too large as well. This observation applies mostly to the noninteracting part of the two-particle spectral function represented by the first contribution to the two-nucleon propagator in Eq. (18). This term also yields a spurious contribution to the cross section for the one-body current contributions at small momenta [26]. The issue of interest here involves the effect of SRC which appear at higher momenta and the problem of spuriosity is not important. The overestimate may be much less severe for the interacting part of the spectral function [second term in Eq. (18)] which yields the genuine SRC contribution to the cross section. In addition, such a factor, representing this overestimate, will be roughly the same for all the low-energy amplitudes involving removal of two protons from the p shell and therefore this uncertainty cancels in the comparison of *relative* magnitudes of amplitudes and cross sections for the low-energy final states in ^{14}C.

The shell-model two-proton removal amplitudes are expanded in terms of relative and c.m. wave functions for the initial state of the knocked-out pair. Summation over the contribution of the various configurations yields the coefficients c in Eq. (13):

$$c^i_{nlSjNL}=\sum_{ab}\sum_\lambda(-)^{L+\lambda+j+S}(2\lambda+1)$$
$$\times\hat j\hat S\hat j_a\hat j_b\begin{Bmatrix} l_a & l_b & \lambda\\ s_a & s_b & S\\ j_a & j_b & J\end{Bmatrix}\langle nlNL\lambda|n_al_an_bl_b\lambda\rangle$$
$$\times\begin{Bmatrix} L & l & \lambda\\ S & J & j\end{Bmatrix}X^i_{abJ}, \tag{19}$$

with the notation $\hat j=\sqrt{2j+1}$ and the nine-j and six-j symbols coming from the angular momentum recouplings involved [26,40].

The most important amplitudes are listed in Table I. It is instructive to note that for these low-lying positive parity states the relative $^1S_0$ wave is combined with a c.m. $L=0$ (for 0^+) or $L=2$ (for 2^+) wave, while the relative ^3P waves occur always combined with a $L=1$ c.m. wave function. This was the basis of the global analysis of the experimental cross section in terms of $^1S_0$ and ^3P removal contributions in Ref. [1]. The amplitudes for the 0^+ states are presented at some length to illustrate the importance of the pairing interaction which mixes the shell-model configurations. Without this interaction, the lowest state would just correspond to the removal of two (dressed) protons from the $p_{1/2}$ shell and the excited 0^+ state to the removal from the $p_{3/2}$ shell. In that case the $^1S_0$ removal cross section would be twice as large for the excited state as for the ground state. Due to the residual interaction the ground state becomes the strongest for $^1S_0$ removal, not only due to the coherent superposition of the p shell configurations but also the deep $0s$ shell and the higher sd and pf major shells contribute. The contribution

from these higher shells is much smaller for the 2^+ states and completely negligible for the 1^+ state.

Another point to be mentioned is that the squares of the amplitudes add up to only about 0.6, as to be expected on the basis of the products of two one-nucleon removal spectroscopic factors $(0.75)^2$.

III. TWO-PROTON KNOCKOUT CROSS SECTIONS

A. Relative magnitude of the contributions from one-body and two-body currents

Of major interest in the $(e,e'pp)$ studies is the question whether one may clearly identify the contributions from one-body and two-body currents and thereby study them separately. The part involving the one-body current is expected to provide then an opportunity to probe SRC. These SRC, induced by the repulsive NN interaction, with a range of typically 0.5 fm, will strongly affect the relative $^1S_0$ wave function, but the short-range repulsion will have only a minor impact on the higher partial waves. For this reason a first inspection of the experimental data from NIKHEF has been made in Ref. [1] to estimate the relative contribution of $^1S_0$ and ^3P pair knockout in the cross sections for the lowest states of ^{14}C. This estimate was based on the comparison of a simple factorization approximation of the cross section with the observed distribution of c.m. momenta of the knocked-out pairs (see also Ref. [17]). Here we present the separate contributions of the $^1S_0$, ^3P_j, and $^1D_2$ relative partial waves to the ^{16}O$(e,e'pp)$ cross sections for the low-lying states in ^{14}C. They are displayed in Fig. 2 for a specific kinematical setting that is included in the aforementioned NIKHEF data, with $E_0=584$ MeV, $\theta=26.5°$, $\omega=212$ MeV, and $q=300$ MeV/c. The kinetic energy of the first outgoing proton T_1' is 137 MeV. The missing energy $E_{2m}=\omega-T_1'-T_2'-T_B'$, where T_2' and T_B' are the kinetic energies of the second outgoing proton and of the residual nucleus, respectively, has been taken in the calculations, for each transition, from a comparison with the experimental spectrum of ^{14}C [44] but for the 2_2^+ state, unidentified in the experimental spectrum, from the calculation of Ref. [26]. The angle γ_1 is $-30°$, on the opposite side of the outgoing electron with respect to $\boldsymbol{q}$. Changing the angle γ_2 on the other side the cross section can be explored at different values of the recoil momentum $\boldsymbol{p}_B$. The relationship between γ_2 and p_B is shown in Fig. 3 for the transition to the ground state of ^{14}C. Only small differences are obtained for the other states, owing to the different value of the missing energy.

In a factorized approach, where final-state interaction is neglected, $\boldsymbol{p}_B$ is opposite to the total momentum of the initial nucleon pair. Thus in this approach the shape of the recoil momentum distribution is determined by the c.m. orbital angular momentum L of the knocked-out pair. This feature is not spoiled by final state interaction, which modifies the pair momentum. In fact in Fig. 2 the shapes of the angular distributions for different transitions and separate contributions of different relative states are determined by the corresponding values of L, indicated in Table I. The shape of the total result is driven by the component which gives the major contribution. Due to final-state interaction there is interference of

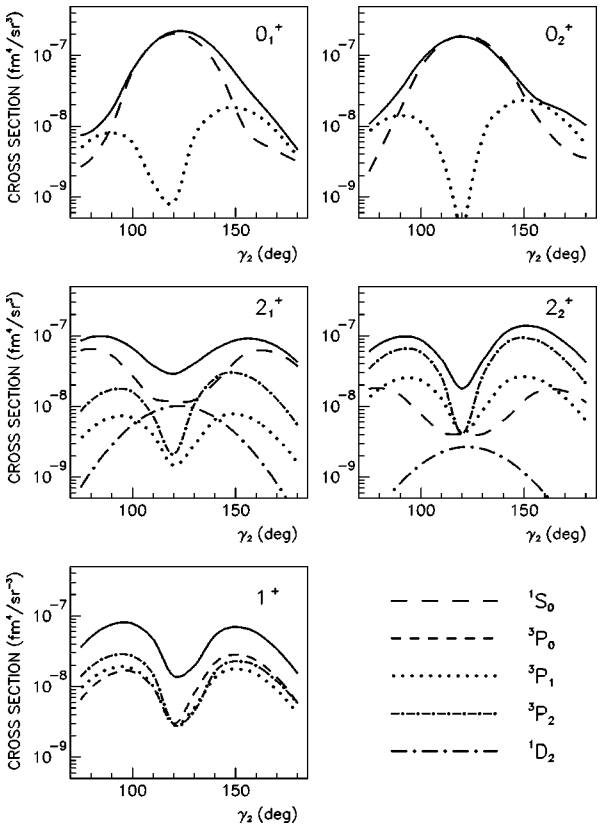

FIG. 2. The differential cross section of the ^{16}O$(e,e'pp)$ reaction as a function of the angle γ_2 for the transitions to the low-lying states in ^{14}C: 0_1^+ ($E_{2m}=22.33$ MeV), 0_2^+ ($E_{2m}=32.08$ MeV), 2_1^+ ($E_{2m}=30$ MeV), 2_2^+ ($E_{2m}=35.47$ MeV), 1^+ ($E_{2m}=33.64$ MeV). $E_0=584$ MeV, $\omega=212$ MeV, $q=300$ MeV/c, $T_1'=137$ MeV, and $\gamma_1=-30°$. The defect functions for the Bonn-A potential and the optical potential of Ref. [46] are used. Separate contributions of different relative partial waves are drawn. The contribution of the $^1D_2$ partial wave is very small for the 0^+ states and omitted from the figure. The solid lines give the total cross sections resulting from the contributions of all the relative states.

different partial waves in the total cross section. In some cases it can be important, but in certain kinematical regions this is of minor importance, because there either one is much stronger than the other.

The figures show that the cross section for the 0^+ ground state, for the 0_2^+, and to a lesser extent also for the 2_1^+ state of ^{14}C, receive a major contribution from the $^1S_0$ knockout,

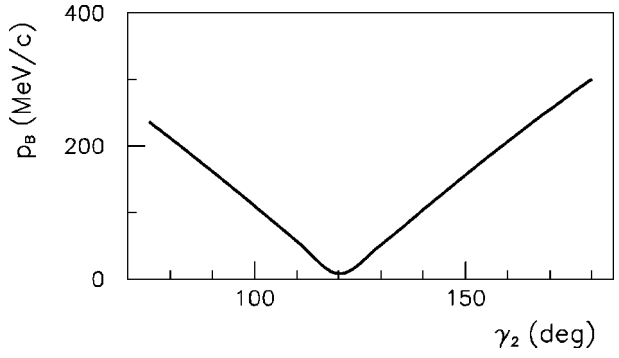

FIG. 3. The recoil momentum p_B as a function of γ_2 in the same kinematics as in Fig. 2.

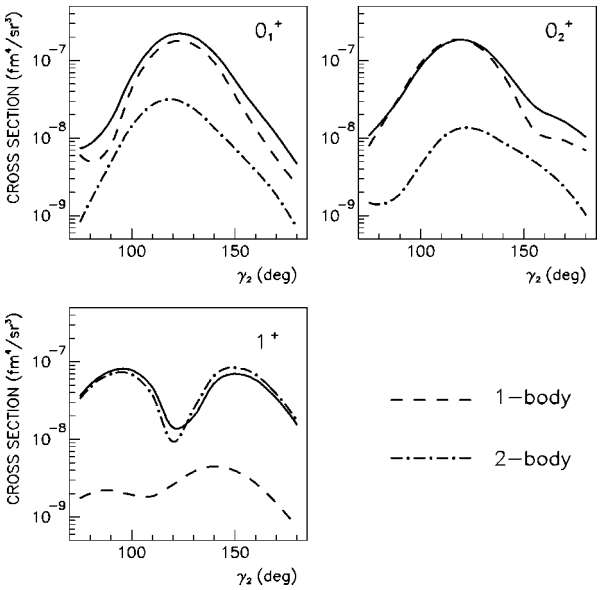

FIG. 4. The differential cross section of the ^{16}O$(e,e'pp)$ reaction as a function of γ_2 for the transitions to the 0_1^+, 0_2^+, and 1^+ states in ^{14}C in the same kinematics as in Fig. 2. Defect functions and optical potential as in Fig. 2. Separate contributions of the one-body and of the two-body Δ current are shown. The solid lines are the same as in Fig. 2.

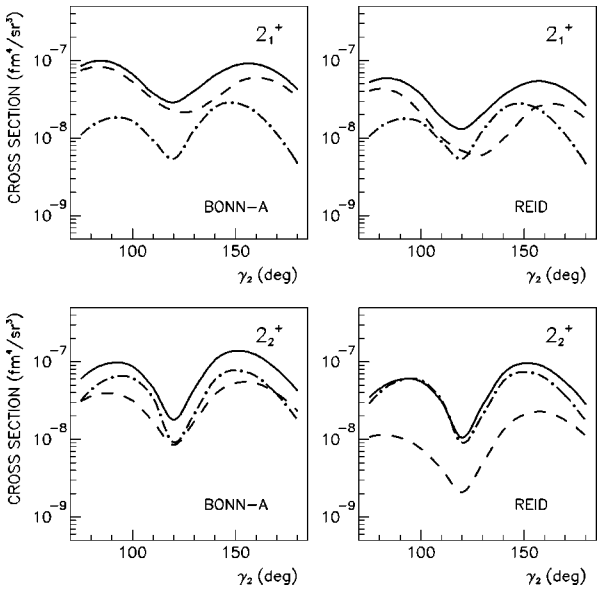

FIG. 5. The differential cross section of the ^{16}O$(e,e'pp)$ reaction as a function of γ_2 for the transitions to the 2_1^+ and 2_2^+ states in ^{14}C in the same kinematics as in Fig. 2. Separate contributions of the one-body and of the two-body Δ current are shown for the defect functions calculated with the Bonn-A and Reid potentials. The solid lines give the total cross sections resulting from the sum of the one-body and of the two-body Δ current. Line convention and optical potential as in Fig. 4.

as opposed to the higher lying states 1^+, where only ^3P waves contribute, and 2_2^+, where the ^3P waves are more prominent. This feature is in agreement with the experimental findings of Ref. [1]. The defect functions used in the calculations of Fig. 2 were those of the Bonn-A potential [26]. The results for the Reid Soft Core potential have a similar qualitatitive behavior for this case and therefore are not presented here. Calculations with the Bonn-C potential have not been performed, but from the shape of the defect functions shown in Fig. 1 we do not expect any significant difference with respect to the results obtained with the Bonn-A potential.

As already mentioned, one may hope that the one-body current and thus correlations yield the dominant contribution to the cross section in some kinematical regions when the knocked-out pair is in a $^1S_0$ state. The knockout of ^3P and higher partial waves will proceed mainly through the two-body Δ current. To illustrate to what extent our calculations support these expectations, we have plotted in Figs. 4 and 5 the separate contributions from the one-body and two-body current to the same total cross section as in Fig. 2. For the 0^+ states the contribution of the one-body current is much larger than that of the two-body current and the angular dependence has the s-wave shape typical of the $^1S_0$ contribution for these states. The results with the Reid defect functions have a similar shape but are a factor of 2 smaller. In fact the range of relative momenta $p_{\rm rel}=|\boldsymbol{p}_1-\boldsymbol{p}_2|/2$ probed in this region is $\approx 1.5\ {\rm fm}^{-1}$, where the ratio of the Bonn-A and Reid $^1S_0$ defect functions is ≈ 1.4, which gives a factor of 2 in the cross section. For larger values of the recoil momentum the s wave becomes smaller, while the p wave becomes relatively more important. In the range of angles between 100° and 140°, where the recoil momentum is small, one may therefore probe correlations in the relative $^1S_0$ wave function.

In sharp contrast to the 0^+ states is the situation for the 1^+ state. It is only reached by the knockout of ^3P pairs and, as expected, the two-body current gives here by far the dominant contribution to the cross section. It will therefore be interesting to identify this cross section for the 1^+, which is known to be at 11.3 MeV excitation energy.

For the 2_1^+ state we find that the one-body current gives a larger contribution than the two-body current, as opposed to the situation for the 2_2^+ state. This may be traced back to the large contribution of the $^1S_0$ partial wave for the 2_1^+, as was shown in Fig. 2. For the 2_2^+ especially $^3P_2$ dominates. However, the predicted dominance of the one-body contribution to the 2_1^+ cross section depends on the defect functions used. This is shown by the comparison between the results obtained with defect functions from the Bonn-A and from the Reid potential in Fig. 5. With the Reid defect functions the one-body current contribution is almost a factor of 2 smaller than for the Bonn-A defect functions. This is not a general statement, but it turns out to be the case for the present kinematics. The cross section calculated with the two-body current is, as expected, only slightly affected by the choice of the defect functions. With the Reid defect functions the amplitudes from one- and two-body currents become of about the same size for the 2_1^+ state and the shape of the total cross section is determined by the interference of the two contributions. A similar result is obtained with the Bonn-A defect functions for the 2_2^+ state.

Next, we show explicitly how the amplitudes for knockout from $^1S_0$ and higher partial waves are influenced by the Δ current. This is plotted in Fig. 6 for the 0_1^+ and 2_1^+ states. The figures illustrate that indeed the $^1S_0$ knockout amplitude is relatively little affected by the inclusion of the Δ current,

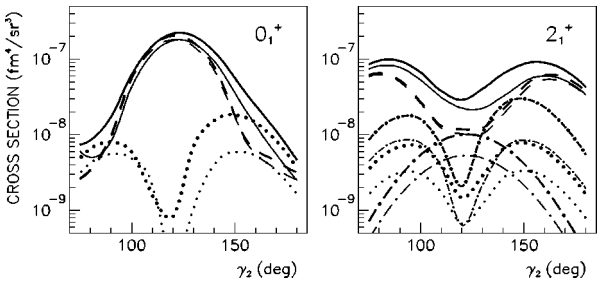

FIG. 6. The differential cross section of the $^{16}O(e,e'pp)$ reaction as a function of γ_2 for the transitions to the 0_1^+ and 2_1^+ states in ^{14}C in the same kinematics and with the same line convention as in Fig. 2. Defect functions and optical potential as in Fig. 2. The thin, mostly lower lines are calculated with the one-body current only.

while this two-body current is a major factor in the knockout of ^3P and ^1D waves. This is a general result that has been obtained also in other kinematical situations. It can be understood if we consider the different role of the excitation and deexcitation part of the Δ current. The excitation current, which has the energy-dependent Δ propagator of Eq. (12), gives for energy transfer above 150 MeV the dominant contribution of the Δ current on ^3P and ^1D waves. The contribution of the excitation current is strongly reduced on a ^1S_0pp pair, where the generally dominant magnetic dipole $NN \leftrightarrow N\Delta$ transition is suppressed because of total angular momentum and parity conservation [45], and becomes in our calculation about the same size or even smaller than that of the deexcitation current, which is generally small. This reduction of the contribution of the Δ current involving the removal of $^1S_0$ pp pairs relative to other states of relative motion was also observed in Ref. [20] for the $^3He(e,e'pp)$ reaction. Thus the contribution of the Δ current, while not zero, is generally small on a $^1S_0$ pp pair, whereas it is dominant on ^3P and ^1D pp pairs. The contribution of the ^1D waves to the total cross section is generally very small. So the proper place to study the two-body Δ current in the $(e,e'pp)$ reaction is where the ^3P knockout dominates, as in the 1^+ and 2_2^+ states, while SRC should be studied in the lowest states, where the $^1S_0$ knockout dominates. Whether indeed one of these is dominant can be verified by inspection of the pair momentum distribution, as was illustrated in Ref. [1].

B. Dependence on the *NN* potential and on the probed range of momenta

In the discussion of Fig. 5 it was already indicated that especially the cross sections due to correlations and the one-body current are sensitive to the defect functions and thereby to the *NN* potential from which these were derived. For the range of relative momenta probed in the cross sections of Figs. 2–6, the $^1S_0$ defect function of the Bonn-A potential is larger than that of Reid. In different kinematical situations it may be just the opposite. This appears to be the case for instance in the kinematics of Ref. [12]. In Fig. 7 it is shown that with that kinematics the contribution of the one-body current to the cross section for 0_1^+ and 2_1^+ is for most angles larger for Reid than for Bonn-A. The range of relative momenta probed here is on the average higher than in Figs. 2–6.

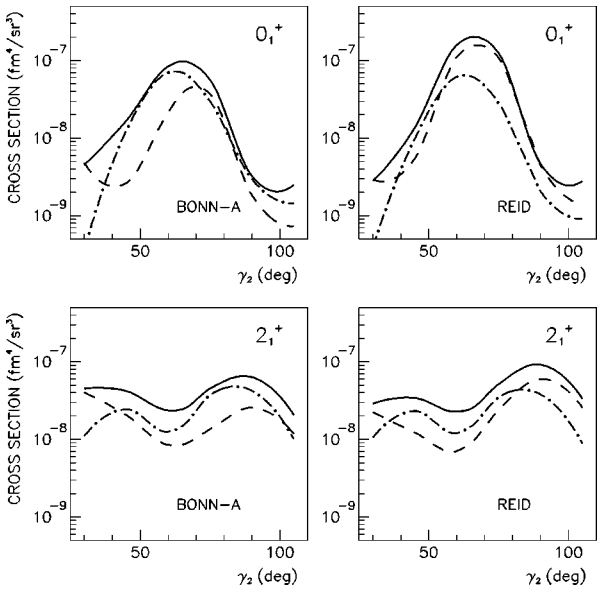

FIG. 7. The differential cross section of the $^{16}O(e,e'pp)$ reaction as a function of γ_2 for the transitions to the 0_1^+ and 2_1^+ states in ^{14}C, now in the same kinematics as in Ref. [12]: $E_0=475$ MeV, $\omega=212$ MeV, $q=268$ MeV/c, $T_1'=68$ MeV, and $\gamma_1=79.2°$. Line convention as in Fig. 4.

Around $\gamma \approx 65°$ the 0_1^+ cross section is probed with $p_{rel} \approx 2.1$ fm^{-1}. For the 2_1^+ state the maximum around $\gamma \approx 90°$ corresponds to $p_{rel} \approx 2.2$ fm^{-1}.

For really high relative momenta, above $p_{rel} \approx 3$ fm^{-1}, the contribution of the one-body current to the cross section will become systematically about a factor of 2 larger for Reid than for the Bonn potentials. This is clear from the momentum dependence of the $^1S_0$ defect wave functions that were shown in Fig. 1. These might be probed in future experiments at TJNAF. Another possibility to discriminate between these potentials could be provided by the separation of structure functions. We discuss an example of this in the next subsection.

C. Separation of the structure functions f_{00} and f_{11} in superparallel kinematics

The experimental separation of structure functions appears in general extremely complicated. The so-called superparallel kinematics, where the knocked-out protons are detected parallel and antiparallel to the transferred momentum $\boldsymbol{q}$, is favored by the fact that only two structure functions, f_{00} and f_{11}, contribute to the cross section, as in the inclusive electron scattering, and, as in that case, they can in principle be separated by a Rosenbluth plot [9]. This kinematical setting has been realized in a recent experiment at Mainz [23]. In this experiment, with an energy resolution of less than 1 MeV, different final states can be separated in the excitation-energy spectrum of the residual nucleus, in particular the 2^+ states at 7.01 and 8.32 MeV. To compare the experimental results with our calculations, however, these two states should be considered as one state, the 2_1^+, which is split up by the coupling to excitations of the ^{16}O core, that are very complicated and not included in our description.

In Fig. 8 we display the cross sections for the 0_1^+ ground state and the 2_1^+ and 1^+ states in the superparallel kinematics

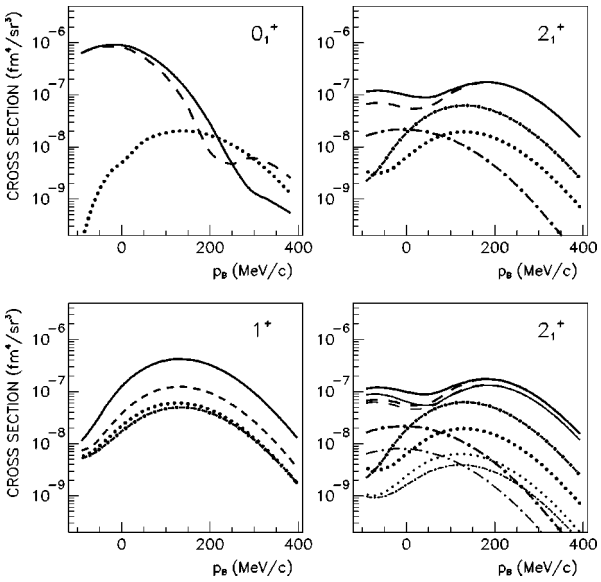

FIG. 8. The differential cross section of the ^{16}O$(e,e'pp)$ reaction as a function of the recoil momentum p_{B} for the transitions to the 0_1^+, 2_1^+, and 1^+ states in ^{14}C in a superparallel kinematics ($\gamma_1=0°$, $\gamma_2=180°$) with $E_0=855$ MeV, $\omega=215$ MeV, and $q=315.89$ MeV/c. The recoil-momentum distribution is obtained changing the kinetic energies of the outgoing protons. Line convention, optical potential, and defect functions as in Fig. 6. Positive (negative) values of p_{B} refer to situations where $\boldsymbol{p}_{\mathrm{B}}$ is parallel (antiparallel) to $\boldsymbol{q}$.

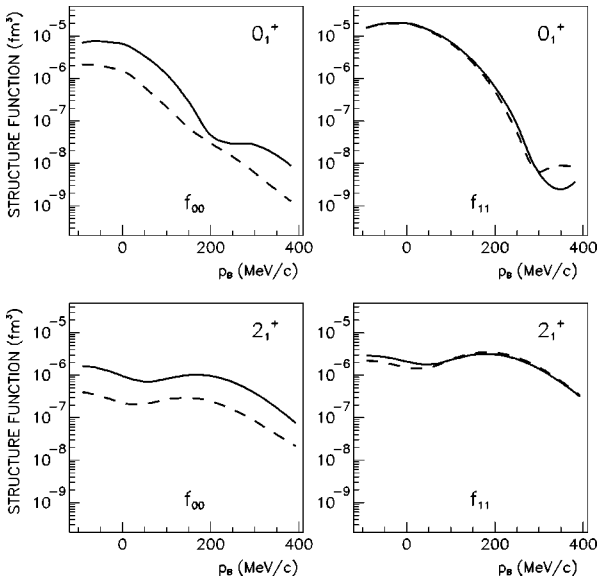

FIG. 9. The structure functions f_{00} and f_{11} of the ^{16}O$(e,e'pp)$ reaction as a function of p_{B} for the transitions to the 0_1^+ and 2_1^+ states in ^{14}C in the superparallel kinematics of Fig. 8. Optical potential as in Fig. 8. The solid and dashed lines are calculated with the defect functions of the Bonn-A and Reid potentials, respectively.

of the Mainz experiment, where $\gamma_1=0°$, $\gamma_2=180°$, $E_0=855$ MeV, $\theta=18°$, $\omega=215$ MeV, and $q=315.89$ MeV/c. The kinetic energy of the outgoing protons is changed in the calculations in order to explore different values of p_{B}. The figures show the decomposition into the different partial waves of the knocked-out pair. The recoil momentum distributions are similar to those shown in Fig. 2. The shapes of the different relative waves are determined by the corresponding value of L. The 0_1^+ state is dominated for low values of p_{B}, up to about 150 MeV/c, by $^1S_0$ knockout. At higher recoil momenta the contributions of $^1S_0$ and $^3P_1$ knockout become of the same order. We observe in this region that the total cross section may be lower than that given by the two separate contributions of $^1S_0$ and $^3P_1$ states, owing to the negative interference of the two contributions. The 2_1^+ state is dominated over the whole range of recoil momenta by $^1S_0$ knockout, whose contribution is about a factor of 4 larger than that of the other relative states. So in this kinematics the 2_1^+ seems to offer the best opportunity to study correlation effects.

We do not display a decomposition into contributions from the one-body and two-body currents here, because the results are conceptually similar to those given in Figs. 4 and 5 and indicate the dominance of the one-body current for the 0^+ and the 2_1^+ states and of the Δ current for the 1^+ state. Moreover, the figures look quite similar to the ones shown here, i.e., the contribution of the one-body current is practically the same as that of the $^1S_0$ removal while higher partial waves come almost exclusively from the two-body current. This is illustrated explicitly for the 2_1^+ state in the last frame of Fig. 8.

Essentially the same results as those shown in Fig. 8, for the Bonn-A defect functions, are obtained with those of the Reid potential. In the latter case the one-body part is about 20% smaller, but otherwise the distributions are quite similar to those of Fig. 8.

A large difference between the results with the defect functions of Bonn-A and Reid potentials appears when a splitting into contributing structure functions f_{00} and f_{11} is made. These results are plotted in Fig. 9. The transverse structure function f_{11} appears to be insensitive to the choice of the defect functions. On the contrary the longitudinal structure function f_{00}, which is entirely due to the one-body current and thus to short-range correlations, is much more sensitive to this choice. This different sensitivity in the considered kinematics is partly due to the effect of the Δ current, which contributes only to f_{11} and is only slightly affected by the defect functions, and partly to the different symmetry behavior of the Coulomb and spin terms of the one-body current. In Fig. 9 f_{00} calculated with the Bonn-A defect functions is typically four times larger than calculated with the Reid defect functions. However, the experimental separation of the structure functions may be difficult, since f_{11} is almost an order of magnitude larger than f_{00} for the 0_1^+ ground state. Also for the 1^+, not shown in the figure, the f_{11} structure function is found to be roughly five times f_{00} with the Bonn-A defect functions and about twenty times f_{00} with the Reid defect functions. Somewhat more favorable is the situation for the 2_1^+ state, since here f_{11} is only three times larger than f_{00} at $p_B\approx 150$ MeV/c, if the prediction with the Bonn-A defect functions turns out to be correct. So this state may offer the best opportunity to determine the longitudinal structure function f_{00} experimentally.

IV. SUMMARY AND CONCLUSIONS

This work represents a combination of state of the art reaction description of the $(e,e'pp)$ reaction together with a

corresponding calculation of the two-nucleon spectral function to produce results for cross sections measured at NIKHEF and Mainz for the ^{16}O target. The description of the reaction includes both one- and two-body contributions to the electromagnetic current. The treatment of final state interactions of the detected protons incorporates distortions (through an optical potential) for the individual particles but not their mutual interaction. Although the latter is expected to be unimportant for the cases of interest, this issue should be further studied in the future. The description of the two-body current involves a proper treatment of the dynamics of the intermediate excitation of the Δ isobar before or after the absorption of the virtual photon. The two-nucleon spectral function (or two-nucleon overlap function) has been obtained from a two-step procedure. The calculation of long-range correlations is performed in a shell-model space large enough to incorporate the corresponding collective features which influence the pair removal amplitude. The single-particle propagators used for this dressed random phase approximation (RPA) description of the two-particle propagator also include the effect of both long- and short-range correlations. In the second step that part of the pair removal amplitudes which describes the relative motion of the pair is supplemented by defect functions obtained from the same G-matrix which is also used as the effective interaction in the RPA calculation.

An important conclusion in this work concerns the predicted selectivity of the $(e,e'pp)$ reaction involving discrete final states. Whereas the lowest 0^+ and 2^+ in ^{14}C are predominantly reached by the removal of a $^1S_0$ pair other states at higher excitation energy mostly involve ^3P removal. The latter pair removal proceeds primarily via intermediate excitation of the Δ isobar whereas the former is dominated by the one-body current mechanism. This feature is responsible for the calculated sensitivity in the cross sections to the treatment of short-range correlations where $^1S_0$ removal dominates. Short-range correlations induced by the Bonn or Reid potential may each yield larger cross sections than the other in certain kinematical domains. As a result, one may be able to study short-range correlations in this reaction successfully provided a sufficiently large set of kinematical conditions is explored including those available at TJNAF. The most promising extraction of the effect of short-range correlations shows up in the longitudinal structure function which may be studied in the so-called superparallel kinematics. Our study demonstrates that an intelligent choice of kinematics in exclusive $(e,e'pp)$ experiments should allow the separation of the effects due to isobar currents and SRC for two nucleons with isospin $T=1$. This success gives rise to the hope that a similar separation between two-body currents and SRC might also be possible in $(e,e'pn)$ reactions. In this case one has to consider the competition between meson-exchange currents and SRC. The emission of a pn pair, however, probes the SRC for $T=0$ which are even stronger due to the presence of the tensor force.

ACKNOWLEDGMENTS

This work forms part of the research program of the Foundation of Fundamental Research of Matter (FOM), which is financially supported by the Netherlands' Organization for Scientific Research (NWO). Additional support was provided by the U.S. National Science Foundation under Grant No. PHY-9602127 and the DFG Programm ''Untersuchung der hadronischen Struktur von Nukleonen und Kernen mit elektromagnetischen Sonden'' under Grant No. Wa 728/3-1 (Germany).

[1] C. J. G. Onderwater *et al.*, Phys. Rev. Lett. **78**, 4893 (1997).
[2] K. Gottfried, Nucl. Phys. **5**, 557 (1958).
[3] W. Kratschmer, Nucl. Phys. **A298**, 477 (1978).
[4] W. Czyz and K. Gottfried, Ann. Phys. (N.Y.) **21**, 29 (1963).
[5] T. de Forest, Jr., Ann. Phys. (N.Y.) **45**, 365 (1967).
[6] C. Ciofi degli Atti, in *Two Nucleon Emission Reactions*, edited by O. Benhar and A. Fabrocini (ETS Editrice, Pisa, 1990), p. 1.
[7] O. Benhar, A. Fabrocini, and S. Fantoni, in *Two Nucleon Emission Reactions* [6], p. 49.
[8] S. Boffi, in *Two Nucleon Emission Reactions* [6], p. 87.
[9] C. Giusti and F. D. Pacati, Nucl. Phys. **A535**, 573 (1991).
[10] C. Giusti, F. D. Pacati, and M. Radici, Nucl. Phys. **A546**, 607 (1992).
[11] S. Boffi, C. Giusti, F. D. Pacati, and M. Radici, *Electromagnetic Response of Atomic Nuclei*, Oxford Studies in Nuclear Physics (Clarendon Press, Oxford, 1996).
[12] C. Giusti and F. D. Pacati, Nucl. Phys. **A615**, 373 (1997).
[13] C. Giusti and F. D. Pacati, Nucl. Phys. **A585**, 618 (1995).
[14] J. Ryckebusch, L. Machenil, M. Vanderhaeghen, and M. Waroquier, Phys. Lett. B **291**, 213 (1992).
[15] J. Ryckebusch, M. Vanderhaeghen, L. Machenil, and M. Waroquier, Nucl. Phys. **A568**, 828 (1994).
[16] J. Ryckebusch, M. Vanderhaeghen, K. Heyde, and M. Waroquier, Phys. Lett. B **350**, 1 (1995).
[17] J. Ryckebusch, Phys. Lett. B **383**, 1 (1996).
[18] J. Ryckebusch, V. Van der Sluys, K. Heyde, H. Holvoet, W. Van Nespen, and M. Waroquier, Nucl. Phys. **A624**, 581 (1997).
[19] R. Carrasco, M. J. Vicente Vacas, and E. Oset, Nucl. Phys. **A570**, 701 (1994).
[20] J. M. Laget, Phys. Rev. C **35**, 832 (1987).
[21] A. Zondervan *et al.*, Nucl. Phys. **A587**, 697 (1995).
[22] L. J. H. M. Kester *et al.*, Phys. Rev. Lett. **74**, 1712 (1995).
[23] G. Rosner, in Conference on Perspectives in Hadronic Physics, edited by S. Boffi, C. Ciofi degli Atti, and M. M. Giannini (World Scientific, Singapore, in press).
[24] P. Bartsch *et al.*, MAMI proposal Nr: A1/1-97.
[25] P. Wilhelm, H. Arenhövel, C. Giusti, and F. D. Pacati, Los Alamos archive nucl-th/9702031, Z. Phys. A (to be published).
[26] W. J. W. Geurts, K. Allaart, W. H. Dickhoff, and H. Müther, Phys. Rev. C **54**, 1144 (1996).
[27] G. A. Rijsdijk, K. Allaart, and W. H. Dickhoff, Nucl. Phys. **A550**, 159 (1992).
[28] W. J. W. Geurts, K. Allaart, W. H. Dickhoff, and H. Müther, Phys. Rev. C **53**, 2207 (1996).

[29] M. Leuschner *et al.*, Phys. Rev. C **49**, 955 (1994).
[30] H. Müther and W. H. Dickhoff, Phys. Rev. C **49**, R17 (1994).
[31] H. Müther, A. Polls, and W. H. Dickhoff, Phys. Rev. C **51**, 3051 (1995).
[32] A. Polls, M. Radici, S. Boffi, W. H. Dickhoff, and H. Müther, Phys. Rev. C **55**, 810 (1997).
[33] R. D. Peccei, Phys. Rev. **176**, 1812 (1968); **181**, 1902 (1969).
[34] D. O. Riska, Phys. Rep. **181**, 207 (1989).
[35] Th. Wilbois, P. Wilhelm, and H. Arenhövel, Phys. Rev. C **54**, 3311 (1996).
[36] B. H. Bransden and R. G. Moorhouse *The Pion-Nucleon System* (Princeton University Press, Princeton, NJ, 1973).
[37] T. A. Brody and M. Moshinsky, *Tables of Transformation Bracket for Nuclear Shell-Model Calculations* (Universidad Autonoma de Mexico, Mexico D.F., 1960).
[38] H. Müther and P. U. Sauer, in *Computational Nuclear Physics*, edited by K.-H. Langanke, J. A. Maruhn, and S. E. Koonin (Springer, New York, 1993).
[39] G. A. Rijsdijk, W. J. W. Geurts, K. Allaart, and W. H. Dickhoff, Phys. Rev. C **53**, 201 (1996).
[40] A. R. Edmonds, *Angular Momentum in Quantum Mechanics* (Princeton University Press, Princeton, NJ, 1957).
[41] P. J. Brussaard and P. W. M. Glaudemans, *Shell-Model Applications in Nuclear Spectroscopy* (North-Holland, Amsterdam, 1977).
[42] A. L. Fetter and J. D. Walecka, *Quantum Theory of Many Particle Physics* (McGraw-Hill, New York, 1971).
[43] A. A. Abrikosov, L. P. Gorkov, and I. E. Dzyaloshinski, *Methods of Quantum Field Theory in Statistical Physics* (Dover, New York, 1975).
[44] F. Ajzenberg-Selove, Nucl. Phys. **A523**, 1 (1991).
[45] P. Wilhelm, J. A. Niskanen, and H. Arenhövel, Nucl. Phys. **A597**, 613 (1996).
[46] A. Nadasen *et al.*, Phys. Rev. C **23**, 1023 (1981).